Electrocatalytic Degradation of Phenolic Wastewater using a Zero-Gap Flow-through Reactor Coupled with a 3D Ti/RuO2-TiO2@Pt Electrode

Yunqing Zhu *, Kaiyue Wen, Bingqing Li,Yirong Hao, Jianjun Zhou

School of Environmental Science and Engineering, Shaanxi University of Science and Technology, Xian 710021, PR China

*Corresponding author: **Yunqing Zhu**

Email address: zhuyunqing@sust.edu.cn

Table S1

Parameters of the pseudo-first order kinetic model for electrocatalytic oxidation of phenol with the zero-gap flow-through reactor.

pollutant	Variables	Range	k (min^{-1})	R^2
phenol	electrolyte	Na$_2$SO$_4$	0.0077	0.9899
		NaCl	0.2562	0.9999
		Blank	0.0046	0.9953
	NaCl (g/L)	4	0.1205	0.9988
		6	0.1675	0.9981
		8	0.2074	0.9981
		10	0.2562	0.9999
	current density (mA/cm^2)	5	0.0100	0.9972
		10	0.2562	0.9999
		15	0.2931	0.9987
		20	0.4718	0.9998
	initial concentration (mg/L)	50	0.2562	0.9999
		100	0.0964	0.9921
		150	0.0630	0.9988
		200	0.0421	0.9997
	pH	3	0.1777	0.9930
		5	0.2554	0.9998
		7	0.2562	0.9999
		9	0.2492	0.9998
		11	0.1316	0.9942
	Flow-through reactor	/	0.2562	0.9999
	Conventional electrolyzer	/	0.0708	0.9938

Table S2

Parameters of the pseudo-first order kinetic model for electrocatalytic oxidation of 4-NP with the zero-gap flow-through reactor.

pollutant	Variables	Range	k (min^{-1})	R^2
4-NP	electrolyte	Na$_2$SO$_4$	0.0361	0.9806
		NaCl	0.1736	0.9734
		Blank	0.0074	0.9863
	NaCl (g/L)	4	0.0780	0.9664
		6	0.0926	0.9543
		8	0.0959	0.9386
		10	0.1736	0.9737
	current density (mA/cm^2)	5	0.0629	0.9567
		10	0.1736	0.9737
		15	0.1773	0.9715
		20	0.1911	0.9680
	initial concentration (mg/L)	40	0.1736	0.9737
		60	0.0852	0.9773
		80	0.0599	0.9587
		100	0.0428	0.9303
	pH	3	0.1736	0.9737
		5	0.1316	0.9525
		7	0.0900	0.9412
		9	0.0425	0.9263
	Flow-through reactor	/	0.1736	0.9737
	Conventional electrolyzer	/	0.1018	0.9788
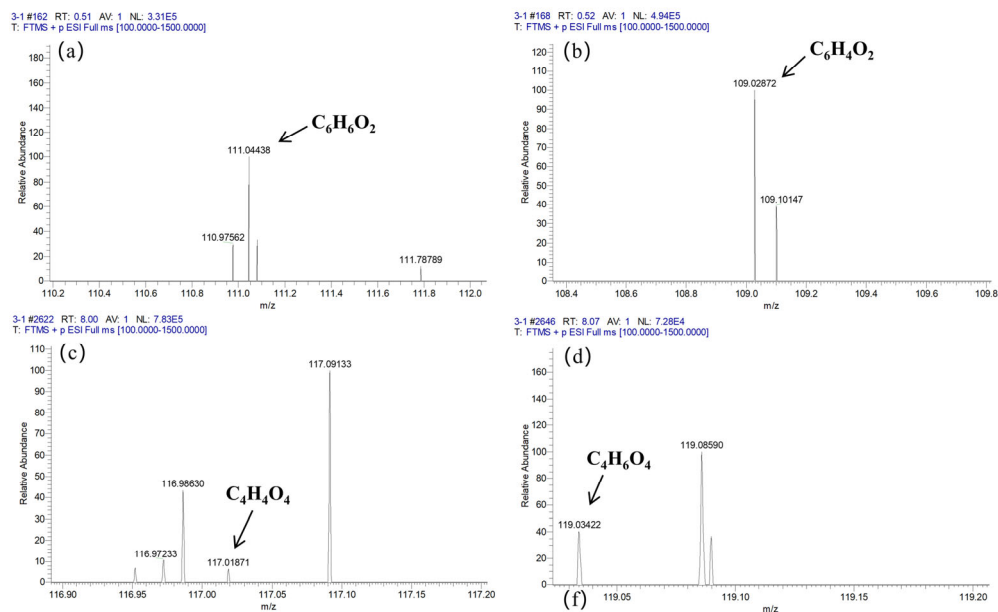
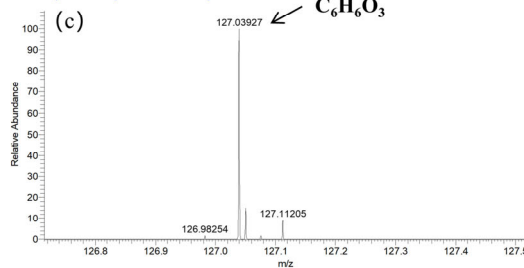**Figure S1.** LC-MS spectrum for mentioned intermediates of phenol.
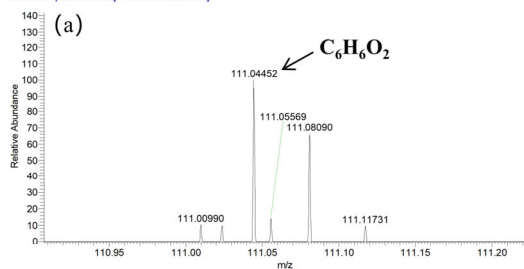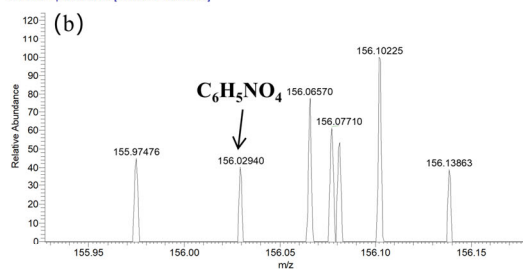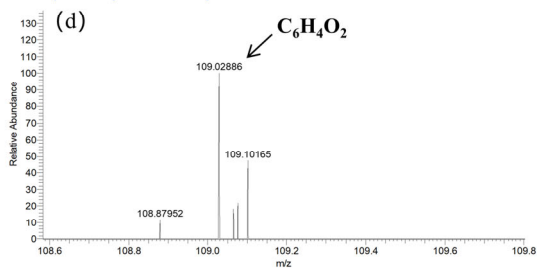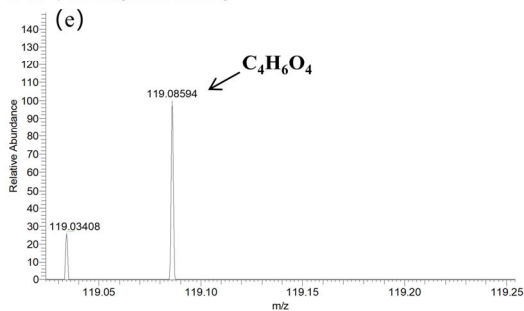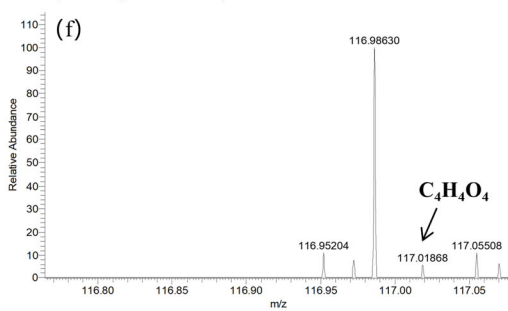
Figure S2. LC-MS spectrum for mentioned intermediates of 4-NP.

Figure S3. Schematic diagram of the electrochemical oxidative degradation process for phenolic pollutants.
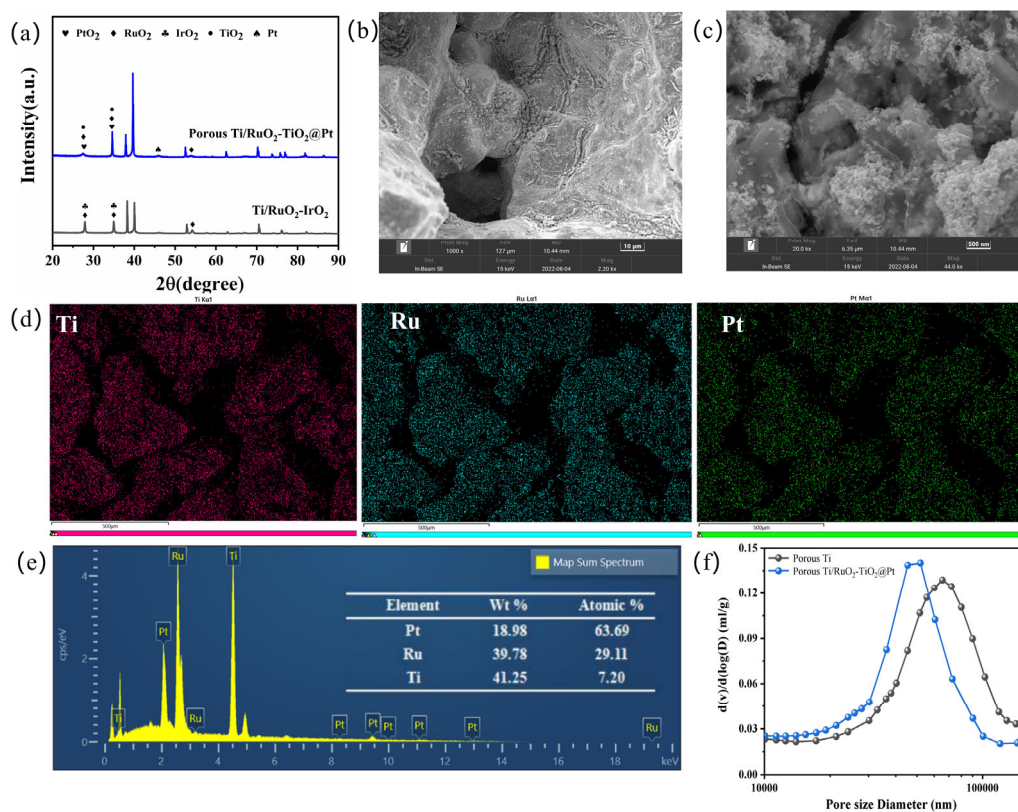
Figure S4. XRD patterns of porous Ti/RuO$_2$-TiO$_2$@Pt (a). SEM images of porous Ti/RuO$_2$-TiO$_2$@Pt at different magnifications (b,c). EDS elemental mappings (d) and EDS spectrum (e) of porous Ti/RuO$_2$-TiO$_2$@Pt. (f) Mercury compression analysis of porous Ti/RuO$_2$-TiO$_2$@Pt.
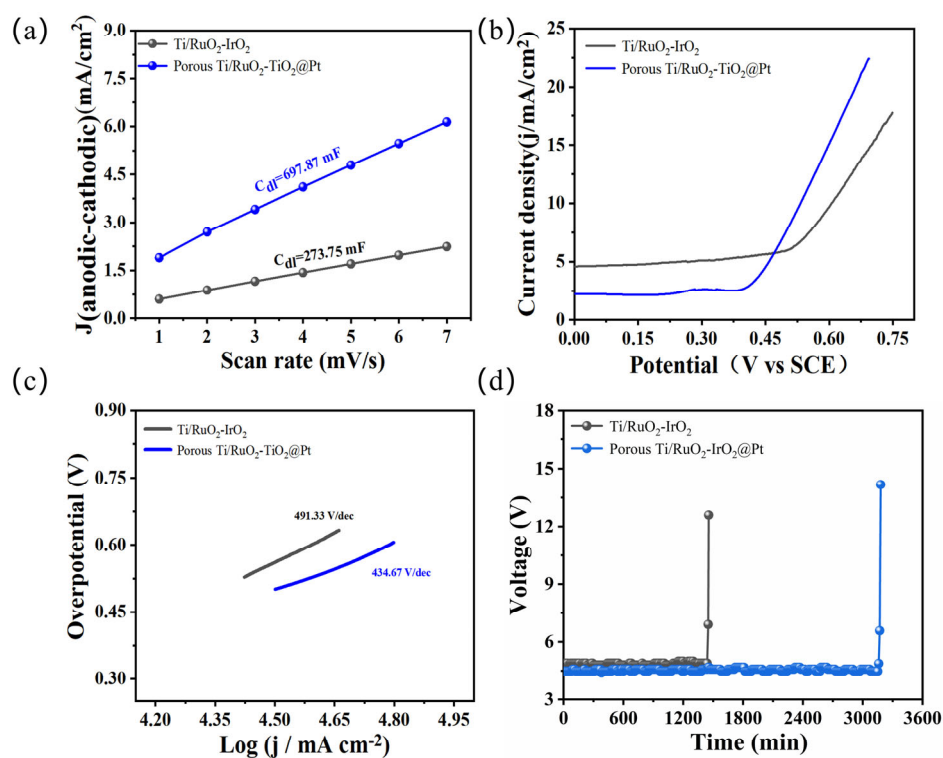
Figure S5. The electric double-layer capacitance diagram (a), LSV curves (b), Tafel curves (c) of porous Ti/RuO$_2$-TiO$_2$@Pt and Ti/RuO$_2$-IrO$_2$ electrodes. (d) Accelerated life test of the prepared electrodes at 2 A/cm^2 in 1 mol/L H$_2$SO$_4$ at 40 °C.
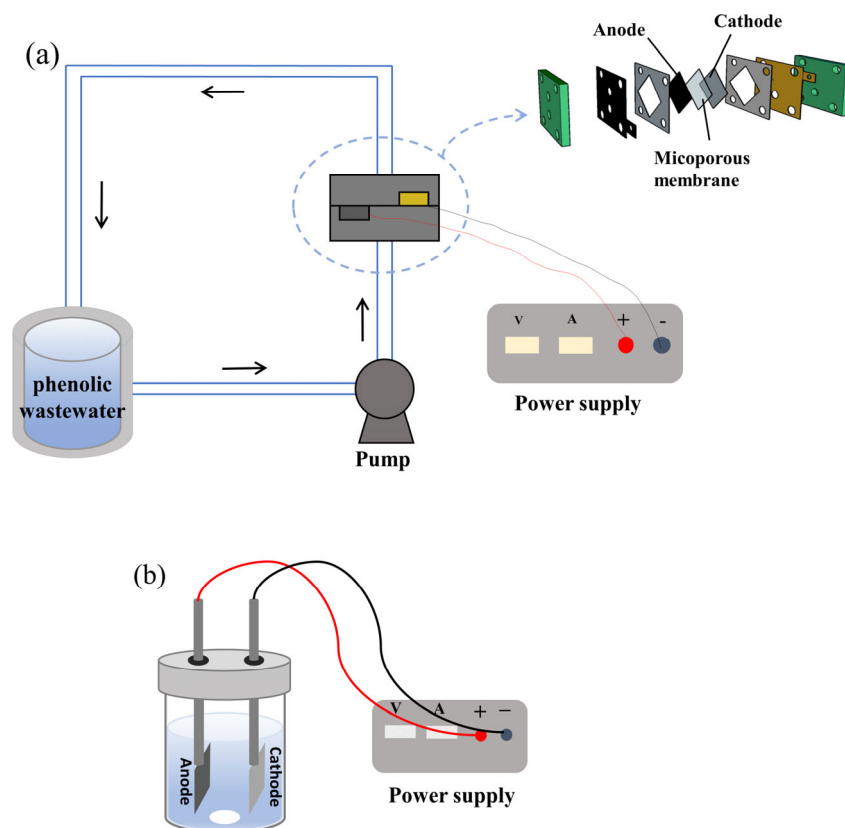
Figure S6. Scheme of the electrochemical systems. (a) zero-gap flow-through reactor; (b) conventional electrolyzer. Anode: 3D porous Ti/RuO$_2$-IrO$_2$@Pt and cathode: porous titanium plate.